Dynamics of End-Linked Poly(propylene sulfide)

Erwan Nicol, Dominique Durand, and Taco Nicolai*

Polymères, Colloides et Interfaces, UMR CNRS, Université du Maine, 72085 Le Mans Cedex 9, France

Received December 8, 1999; Revised Manuscript Received May 31, 2000

ABSTRACT: Poly(propylene sulfide) (PPS) was end-linked using diisocyanate to form polycarbamothioate. The effect of end-linking on the glass transition, the viscoelasticity, and the dielectric permittivity was studied using dielectric (DS) and mechanic spectroscopy (MS). DS showed that the mobility of about 15 PPS segments is reduced by the presence of a carbamothioate link. The present results can be compared with those obtained on polyurethane which is formed by linking poly(propylene oxide), also known as poly(propylene glycol). The interpretation of the present system is easier because PPS does not have a parallel dipole moment and does not show an effect of hydrogen bonding.

Introduction

In the past few years we have conducted an extensive investigation of the dynamic mechanical properties of polyurethane produced by polycondensation of poly(propylene oxide) (PPO) and a diisocyanate.[1−5] We have used both linear and three-armed star PPO. In the case of star PPO, gels are formed while if linear PPO is used, entangled melts are formed. For one star PPO we have studied the system in detail as a function of the connectivity extent either in situ at different reaction extents[1] or at complete reaction by varying the ratio, *r*, of isocyanate groups to hydroxyl groups.[3,4] The effect of varying the molar mass of the precursors was investigated for fully end-linked systems, i.e., $r = 1$ and after complete reaction.[5]

The dynamical properties of the precursor PPO were investigated using dielectric spectroscopy (DS)[6] and mechanic spectroscopy (MS),[7] i.e., by measuring the frequency dependence of the shear modulus. PPO is one of the very few polymers that contains a dipole moment parallel to the chain backbone.[8] This property offers the possibility to measure the end-to-end vector fluctuations of the polymers with DS. As a consequence of the synthesis method, the parallel dipole moment is inverted at the center of both linear and star PPO, and thus linear PPO is best considered as a star with two arms. When PPO is end-linked with diisocyanate, the direction of the dipole is inverted at each urethane link, which means that DS is only sensitive to the fluctuations of the end-to-end vector of the arms.

A direct comparison of these fluctuations for end-linked linear and star PPO with the same arm length showed that the end-to-end vector fluctuations are identical in entangled melts and gels.[9] In this study the arm length was equal to the entanglement length. We found that the slowest relaxation time that characterizes this fluctuation is the same as for the precursor polymers. However, the loss peak of the dielectric permittivity (ϵ'') at higher frequencies was broader after end-linking for both linear and star PPO. Since a large PPO precursor was used in this study, the relative contribution of the urethane links to the total dipole moment is small. Thus, it is clearly the dynamics of the PPO segments that are modified by end-linking. On the other hand, it was not clear whether it is the component of the dipole moment parallel or perpendicular to the polymer backbone which is modified. The broadening seen in DS was not observed with MS where only a weak broadening of the α-relaxation was seen.

Recently, we compared the dynamics of linear poly(propylene sulfide) (PPS) and PPO using DS and MS.[10] The difference between these polymers is that all oxygen atoms in PPO are replaced by sulfur in PPS. The strength of hydrogen bonds is very much reduced when oxygen is replaced by sulfur.[14] For this reason PPS shows the characteristic decrease of the glass transition temperature (T_g) at lower molar mass observed for most polymers, while PPO shows only a weak finite size effect on T_g due to hydrogen bonding of the chain ends. For PPS the relaxation of the end-to-end vector fluctuations is not seen in DS, which means that PPS does not have a measurable component of the dipole moment parallel to the polymer backbone. Despite these differences, the dynamics of PPS and PPO are very similar.

Like PPO, PPS can be end-linked using a diisocyanate to form an entangled melt of polycarbamothioate (PCT):

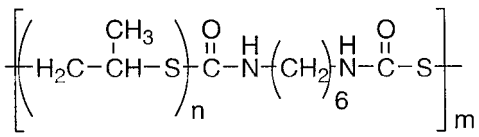

We will show below that the dynamics of end-linked PPS measured by MS are very similar to those of end-linked PPO reported in ref 5. This means that using PPS we can study the influence of end-linking on the relaxation of the dielectric permittivity without the contribution of a component of the dipole moment parallel to the chain backbone. This investigation is necessary for a proper understanding of the relaxation of the dielectric permittivity for polyurethane melts and gels, which will be reported elsewhere.

Experimental Section

Sample Synthesis and Characterization. The synthesis method of the precursor PPS samples is described in ref 12. The characterization of the samples used for this study is reported in ref 10; see Table 1. Polycarbamothioates were formed by polycondensation of thiol end-capped PPS with hexamethylene diisocyanate (HMDI). To obtain fully end-linked systems, the ratio of isocyanate groups to hydroxyl groups, r = [NCO]/[SH], needs to be unity. The amount of HMDI needed to obtain $r = 1$ was calculated on the basis of the molar mass of the samples assuming full functionalization.

10.1021/ma992063b CCC: $20.00
Published on Web 12/08/2000

Table 1. Sample Characteristics

	M_n precursor (kg/mol)	M_w/M_n precursor	DP_n PCT	DP_w/DP_n PCT	T_g (K)	T_{gv} (K)
S1	0.63	1.09	7.3	2.68	244	240
S2	0.9	1.11	14.3	3.07	242	238
S3	1.6	1.19	6.6	2.25	238	233
S4	2.9	1.10	4.3	2.07	236	231.5
S5	6.1	1.14	6.0	2.54	237	231.5

By analogy with the isocyanate−hydroxyl reaction,[13] dibutyl tin dilaurate was added to catalyze the isocyanate−thiol reaction. After mixing and complete homogenization of the components, the samples were cured at 50 °C until complete consumption of the isocyanate groups.

The end-linked samples were characterized using size exclusion chromatography (SEC). We have used two sets of columns: Polymer Laboratories MIX-C 5μm, 600 × 7.5 mm and E-lin 10μm and MIX-B 10μm, each 600 × 7.5 mm. The elution liquid is THF using a flow rate of 1 mL/min. The degree of polymerization was calculated as the ratio of the molar masses before and after end-linking. Values of the number-average degree of polymerization (DP_n) and the polydispersity index (DP_w/DP_n) are given in Table 1.

Calorimetric glass transition temperatures were measured using differential scanning calorimetry (DSC) with a reproducibility of ±2 deg. The samples were cooled rapidly to 150 K and then heated at a rate of 10 deg/min. Values of T_g taken as the midpoint of the transition are summarized in Table 1.

M**echanic Spectroscopy**. Dynamic shear measurements were made on a Rheometrics RDA II dynamic spectrometer using parallel-plate geometry at temperatures between 200 and 340 K. The so-called hold mode was used where the gap is corrected for temperature variations of the sample volume. The plate size (diameters 25, 8, and 4 mm) and the imposed deformation (0.1−100%) were adjusted to obtain an accurate torque response while remaining in the linear regime. The shear modulus could be measured in the range $10-10^9$ Pa. We were able to measure very large moduli by using a relatively large sample thickness (2−2.5 mm) in combination with a small plate size. The range of frequencies, f, used was $2 \times 10^{-3}-20$ Hz. Temperatures were measured using a thermocouple close to the lower plate. The temperature was stable within ±0.2 K over the whole range used in this study (200−350 K).

Dielectric Spectroscopy. Measurements of the complex dielectric permittivity were made with broad-band dielectric spectroscopy equipment from Novocontrol GmbH. Measurements were made in the frequency range from 10^{-1} up to 10^6 Hz. The samples were kept between two gold-plated stainless steel plates of 20 or 40 mm in diameter with a gap varying between 30 and 500 μm. The sample cell was placed in a cryostat, and the sample temperature was regulated with an accuracy of ±0.1 K and measured with a PT100 sensor in the lower plate of the sample capacitor.

Results

Glass Transition Temperature. The calorimetric glass transition temperatures are plotted in Figure 1 as a function of $1/M_n$, where M_n is the number-average molar mass of the precursors. For comparison, we also show the values before end-linking which were reported in ref 10. (Note that in ref 10 the results on PPS are shown as a function of the weight-average molar mass and not as a function of the number-average molar mass as was written in the text.) Before end-linking we find the expected linear decrease of T_g with $1/M_n$ as observed for most polymers: $T_g = 237 - 1.86 \times 10^4/M_n$. End-linking has two effects on the T_g: (1) it eliminates the free end effect which causes T_g to decrease with decreasing molar mass, and (2) it produces an increase of T_g by the introduction of carbamothioate links. (The volume fraction of carbamothioate links increases approximately linearly with $1/M_n$.) The net result is a weak approximately linear increase of T_g with $1/M_n$: $T_g = 235 + 6.14 \times 10^3/M_n$. For PPO the first effect is very small compared to PPS because the mobility of free ends in PPO is much reduced by hydrogen bonding. On the other hand, the second effect is stronger in PPO than in PPS. Apparently, urethane links have a more important hardening effect than carbamothioate links.

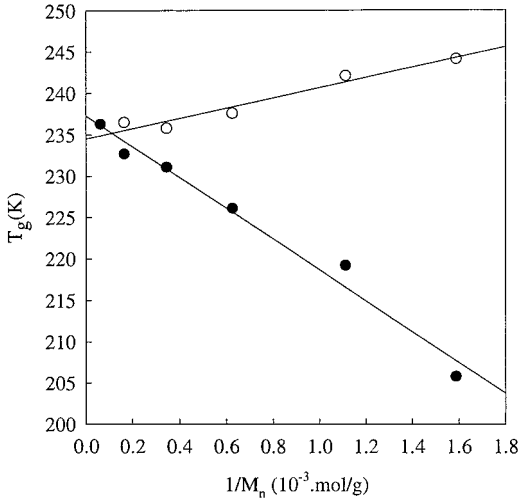

Figure 1. Molar mass dependence of the glass transition temperature of PPS before (filled circles) and after (open circles) end-linking.

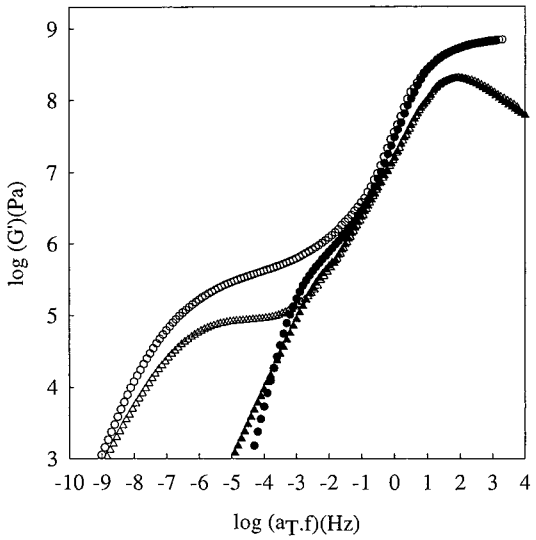

Figure 2. Master curves of the storage (circles) and loss (triangles) shear modulus of sample S5 before (filled symbols) and after (open symbols) end-linking with $T_{ref} = T_{gv} + 5$ K.

Mechanic Spectroscopy. Figure 2 shows the effect of end-linking on the frequency dependence of the loss (G'') and storage (G') shear modulus for S5. The master curves were obtained by time−temperature superposition with $T_{ref} = T_{gv} + 5$ K. T_{gv} is defined as the temperature where the maximum loss shear modulus (G''_m) occurs at angular frequency $\omega = 1$ rad/s and may be considered as an alternative definition of the glass transition temperature. T_{gv} is about 5 deg lower than T_g and is obtained with much better accuracy; see Table 1. The data show the segmental relaxation (α-relaxation) at higher frequencies and the conformational relaxation at lower frequencies.

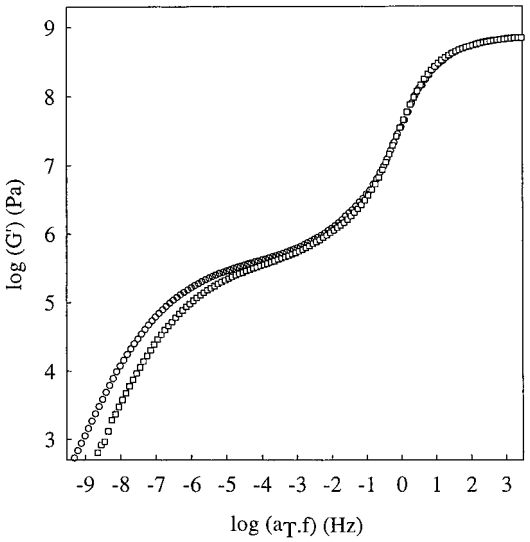

Figure 3. Comparison of master curves of the storage shear modulus of end-linked PPS (circles) with end-linked PPO (squares). The average number of segments of the precursors was 82 for PPS and 70 for PPO. The average number of precursors in the end-linked systems was 6.0 for PPS and 4.8 for PPO.

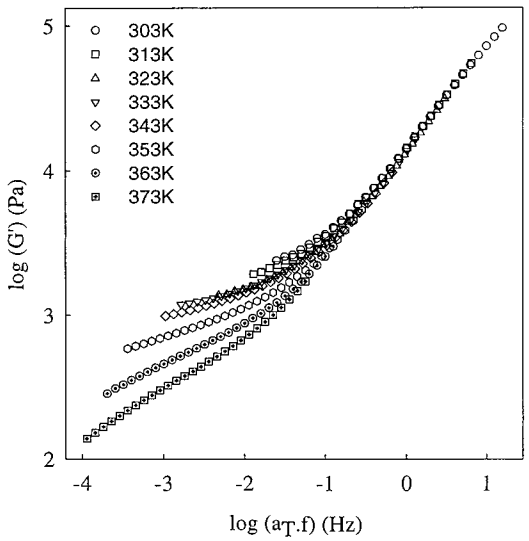

Figure 4. Frequency dependence of G' for end-linked sample S4 at different temperatures indicated in the figure.

As was reported earlier[11] for a number of different polymers, the temperature dependence of the segmental relaxation and the conformational relaxation of PPS are slightly different. The effect is the same for all PPS samples both before and after end-linking. It is identical to that observed for PPO and is discussed in detail in refs 6 and 7. Master curves can nevertheless be constructed by selecting a reference temperature at which both modes are clearly visible and superimposing data obtained at $T < T_{ref}$ at high frequencies and data obtained at $T > T_{ref}$ at low frequencies; see ref 7 for details. The master curves look slightly different for different choices of T_{ref}, but different samples may be compared if we choose T_{ref} at the same distance from T_{gv}.

The effect of end-linking is mainly on the conformational relaxation. The molar mass of S5 is close to that needed for entanglements, $M_e \approx 4$ kg/mol, and its conformational relaxation can be described in terms of Rouse normal modes. After end-linking the molar mass is increased, and the terminal relaxation time (τ_T) is much slowed down by the effect of entanglements. However, the temperature dependence of τ_T is not influenced by end-linking. The number of precursor PPS per PCT, and thus the absolute value of τ_T, is strongly dependent on the stoichiometric ratio of isocyanate groups to thiol groups. Theoretically, if $r \rightarrow 1$, the molar mass of PCT diverges. However, the degree of polymerization (DP_n) is already quite small if r is a few percent different from unity. The experimental uncertainty of r explains the variation of DP and the rather low values. Consequently, the terminal relaxation time after end-linking varies for the different samples and is not correlated to that of the precursors. See ref 5 for a more detailed discussion of this issue in the context of end-linked PPO.

Figure 3 shows that the frequency dependence of the shear modulus is very similar for PCT and PU if they have similar size precursor and degree of polymerization. However, some PCT samples show a striking effect at low temperatures and frequencies which was not observed for PU. Contrary to PU, these samples do not flow at room temperature, and the shear modulus does not reach the flow regime where $G' \propto f^2$ and $G'' \propto f$ at high temperatures. Instead, we observe a much weaker frequency dependence tending to a plateau for G'; see Figure 4. The level of this plateau depends on the temperature and sample history. It increases slowly with time at a given temperature, and at long times the plateau modulus decreases with increasing temperature as shown in Figure 4. We believe that this phenomenon is due to clustering of carbamothioate links, which act as physical cross-links. Hydrogen bonding is a possible reason for the clustering, but in that case one might expect a similar phenomenon for PU. Heating to $T >$ 100 °C destroys the clusters, but they re-form upon cooling. We did not observe this effect for the largest and the smallest PPS samples. For the largest PPS the concentration of carbamothioate links is small, which might explain why the effect is much reduced. We do not know why the effect is absent for the smallest sample. The clustering of carbamothioate links does not influence the measurements at low temperatures because the systems are rapidly cooled from high temperatures and the kinetics of the clustering is very slow. In addition, the fraction of carbamothioate links involved is small so that it does not influence the mechanical response at moduli above 10^4 Pa; see Figure 4.

In Figure 5 we show G''/G''_m as a function of $\log(f/f_m)$ for the end-linked samples. In this representation we observe mainly the loss peak which characterizes the α-relaxation. In ref 10 we have shown that the results for the precursors are independent of the molar mass and are well described by a stretched exponential relaxation in the time domain: $G(t) \propto \exp(-(t/\tau_r)^{\beta})$ with $\beta = 0.47$, for $f < 20f_m$. The solid line in Figure 5 represents this stretched exponential relaxation in the frequency domain. The effect of end-linking is a broadening of the peak for lower molar mass samples similar to what was observed earlier for end-linked PPO.[5]

The temperature dependence of the segmental relaxation time can only be studied over a narrow temperature range, due to the limited dynamical range of the rheometer used in the experiment. Over this small range, the temperature dependence of f_m superimposes if plotted as a function of $T - T_{gv}$; see Figure 10. In this representation the effect of the glass transition temper-

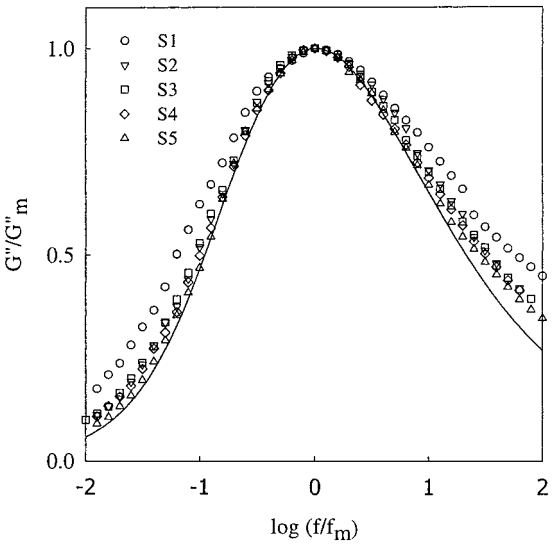

Figure 5. G''/G''_{max} as a function of $\log(f/f_m)$ for end-linked PPS samples with different molar masses. The solid line represents a stretched exponential relaxation in the frequency domain with $\beta = 0.47$.

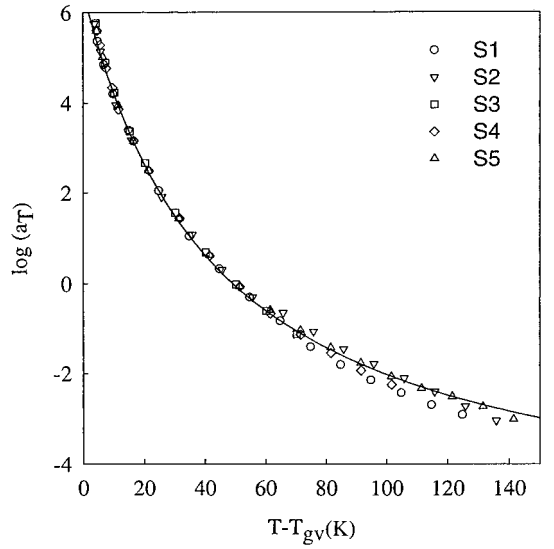

Figure 6. Temperature dependence of the low-frequency shift factors used to obtain the master curves. The solid line represents the results obtained for the precursors.

atures is removed, which allows for a better comparison between samples with different T_g. The dashed line through the data represents the results for the precursors[10] which shows that the temperature dependence is the same before and after end-linking after correction for the different glass transition temperatures. The same observation was reported earlier for PPO.[3]

The temperature dependence of the conformational relaxation can be obtained over a much wider range using time−temperature superposition. In Figure 6 the shift factors (a_T) are plotted as a function of $T - T_{gv}$. In this representation the temperature dependence of a_T is almost the same for all samples and close to that of the precursors indicated by the solid line. The shift factors of the sample S2 at high temperatures may be somewhat influenced by the effect of clustering of carbamothioate links on the shear modulus. We do not show the absolute values of the terminal relaxation times, because, as was mentioned above, they are very sensitive to the amount of added linking agent and are not correlated with those of the precursors.

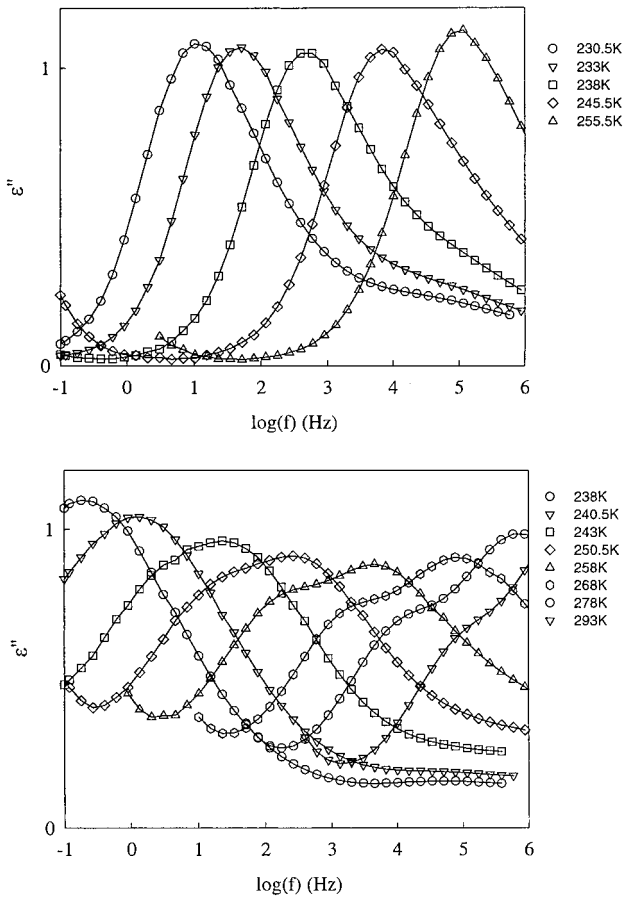

Figure 7. Frequency dependence of ϵ'' for sample S3 before (top) and after (bottom) end-linking at different temperatures indicated in the figure. At these temperatures one mainly observes the α-relaxation.

Dielectric Spectroscopy. In Figure 7 we compare the frequency dependence of ϵ'' for S3 before and after end-linking over a range of temperatures. PPS melts show two relaxation processes: the α-relaxation and the β-relaxation, which merge at high temperatures. The upturn at low frequencies is caused by the conductivity due to the presence of charged impurities. The increase of the peak height at high temperatures is caused by the increasing influence of the merging β-relaxation. In ref 10 we have shown that the shape of the α-relaxation of the precursors before end-linking is independent of the temperature.

End-linking causes an additional relaxation process (α′-relaxation) to appear in the spectrum which merges with the α-relaxation at low temperatures. In Figure 8a we compare the spectra at $T = T_{gv} + 20$ K of five samples with precursor molar masses ranging from 0.63 to 6.1 kg/mol. The presence of two modes slower than the β-relaxation is best seen for the sample S3 because the contributions happens to be about equal. For the other samples one of the modes dominates and the effect of the second mode is only seen as a broadening of the peak. For polycarbamothioates made with higher molar mass samples (S4 and S5) the α-relaxation dominates, and the broadening is toward low frequencies. When lower molar mass PPS (S1 and S2) is used, the α′-relaxation dominates and the broadening is toward high frequencies. The data can be fitted to a sum of two Havriliak−Negami functions, but in view of the large overlap of the two modes the results of such a fit are not necessarily representative of the two relaxation

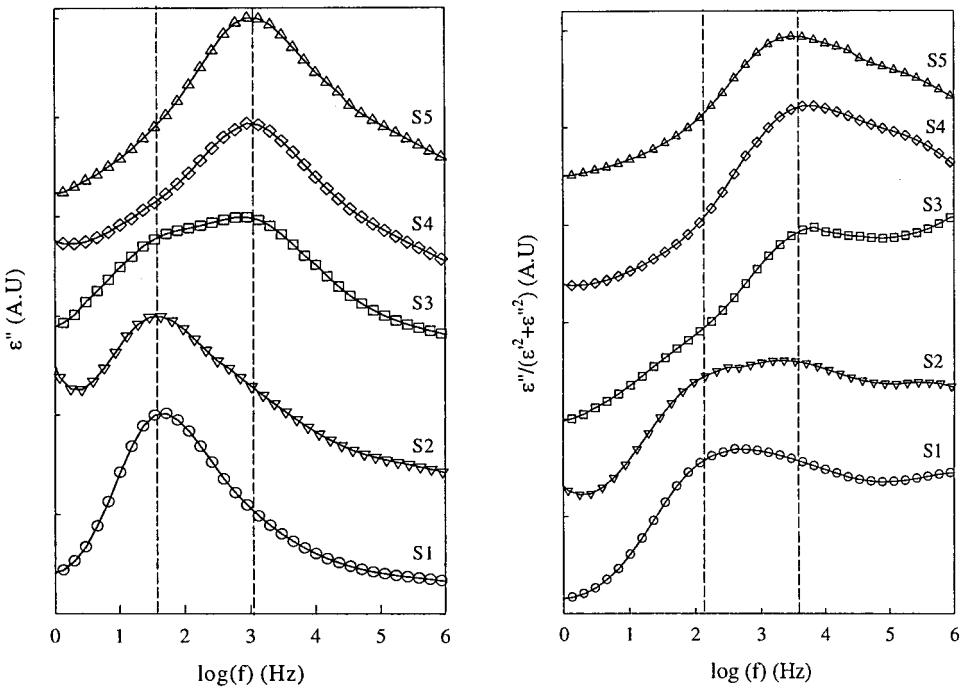

Figure 8. (a) Comparison of the frequency dependence of ϵ'' for end-linked PPS with different molar masses at $T = T_{gv} + 20$ K. The dashed lines indicate the position of the two relaxation modes. (b) Different representation of the same data as shown in (a).

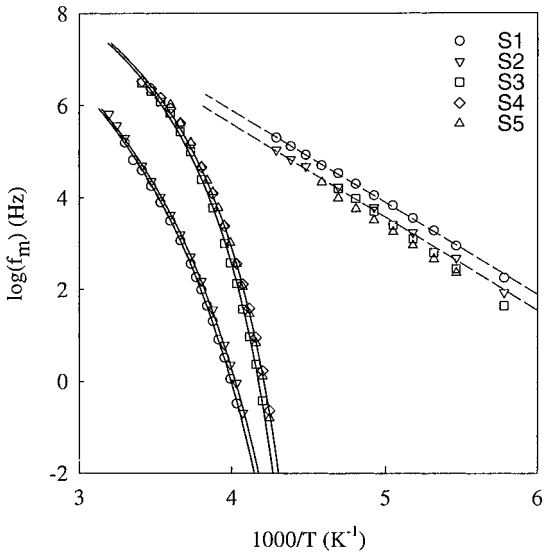

Figure 9. Arrhenius representation of the temperature dependence of the peak position of ϵ'' at low (α-relaxation) and high (β-relaxation) frequencies for end-linked PPS with different molar masses indicated in the figure. The solid lines are fits to the VFT equation (see text), while the dashed lines have the same slope, which corresponds to $E_a = 37 \pm 1$ kJ/mol.

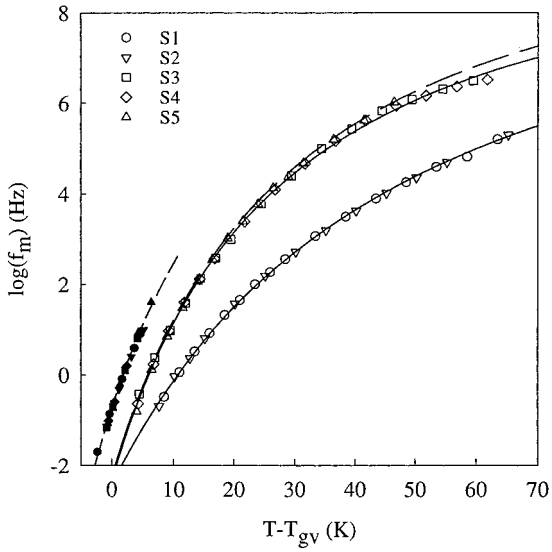

Figure 10. Plot of the loss peak position in DS (open symbols) and MS (filled symbols) as a function of $T - T_{gv}$ for end-linked PPS with different molar masses indicated in the figure. The solid lines are fits to the VFT equation (see text), while the dashed lines represent the results for the precursors.

processes. Figure 8b shows the same data in a different representation which emphasizes the relaxation at high frequencies. In this representation the α- and α′-relaxation have about the same amplitude for S2. For $f > 10^5$ Hz the β-relaxation becomes visible.

In Figure 9 we show in an Arrhenius representation the temperature dependence of the peak position (f_m), i.e., the frequency where ϵ'' is maximum. The data can be fitted to the empirical Vogel−Fulcher−Tamman equation:

$$\log(f_m) = \log(f_\infty) - \frac{B}{T - T_0} \qquad (3)$$

The temperature dependence is qualitatively different for the high (S3, S4, and S5) and low molar mass samples (S1 and S2). The difference is even more evident if we remove the effect of the glass transition temperature by plotting the data as a function of $T - T_{gv}$; see Figure 10. In this representation the shift factors of the high molar mass samples superimpose to form one curve and those of the low molar mass samples to form another. Clearly, f_m represents the α-relaxation for the three higher molar mass samples and the α′-relaxation for the two lower molar mass samples. For the three higher molar mass samples we obtain $B = 355$, $T_0 = T_{gv} - 27.3$, and $\log(f_\infty) = 10.7$, and for the two lower molar mass samples we obtain $B = 643$, $T_0 = T_{gv} - 48.0$, and $\log(f_\infty) = 11.0$. The dashed line in Figure 10

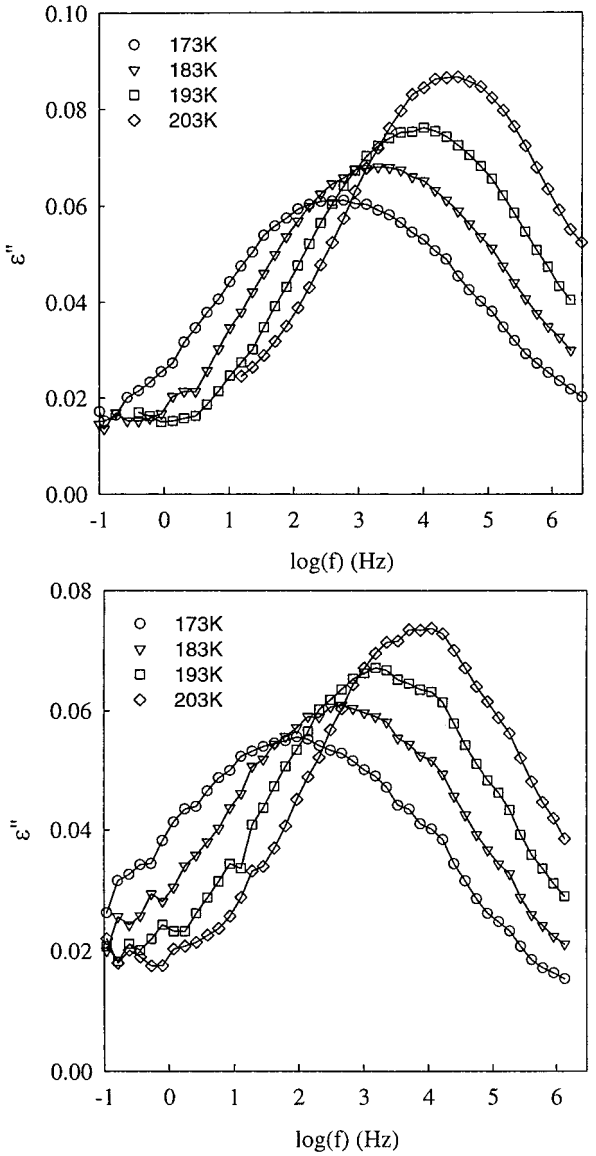

Figure 11. Frequency dependence of ϵ'' for sample S2 before (top) and after (bottom) end-linking at different temperatures indicated in the figure. At these temperatures one mainly observes the β-relaxation.

represents the behavior of the precursors and shows that it is almost identical to that after end-linking for the high molar mass samples. We can therefore identify the α-relaxation as the relaxation of nonmodified dipoles and the α′-relaxation as the relaxation of dipoles that are modified by end-linking. The relative dielectric strength of the modified compared to nonmodified dipoles increases with decreasing molar mass of the precursor PPS.

For S3 we can distinguish the two modes more clearly because, as mentioned above, they happen to have about the same strength. The spectra at different temperatures for this sample show that the relative strength of the modes is not or only weakly temperature dependent; see Figure 7. (The increase of the fast mode at high temperatures is due to merging with the β-relaxation.) The experimental results do not allow for a precise positioning of the slow mode, but the distance on the frequency scale between the two modes in Figure 7 is consistent with that obtained for different samples shown in Figure 10. Figure 10 shows that the distance between the two modes varies with temperature, but

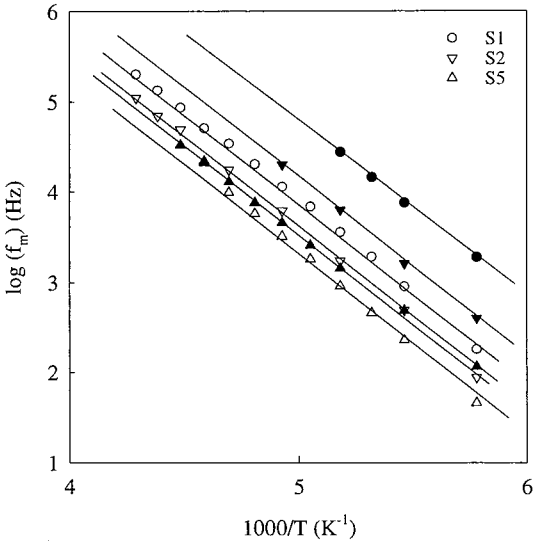

Figure 12. Temperature dependence of the peak position of ϵ'' at high frequencies (β-relaxation) for PPS with different molar masses before (filled symbols) and after (open symbols) end-linking. The solid lines have the same slope which corresponds to $E_a = 37 \pm 1$ kJ/mol.

not with the molar mass of precursor PPS. The dashed lines in Figure 8 indicate the position f_m of the two modes at $T = T_{gv} + 20$ K. Clearly, even if only one mode can be distinguished, the position of the other mode is coherent with the broadening effect.

The β-relaxation is only weakly modified by end-linking. This is illustrated in Figure 11 where we compare the loss peak of sample S2 at several low temperatures before and after end-linking. The loss peak broadens with decreasing temperature and the amplitude decreases. We showed in ref 10 that for PPS the data at different temperatures superimpose if we plot $\epsilon''/\epsilon''_{max}$ as a function of $\log(f/f_m)/\Delta$ where Δ is the half-width of the peak. Both the width and the amplitude of the β-relaxation of the precursor are independent of the molar mass. We found that end-linking does not modify the shape of the β-relaxation loss peak even for the smallest sample.

The β-relaxation has an Arrhenius temperature dependence with an activation energy, $E_a = 37 \pm 1$ kJ/mol, independent of the molar mass of the precursors; see Figure 9. The temperature dependence of f_m before and after end-linking is compared in Figure 12 for three samples. We showed in ref 10 that for PPS the apparent activation energy of the β-relaxation is independent of the molar mass but that the absolute values of f_m are correlated with the glass transition temperature and thus the α-relaxation. The two modes merge at about 10^7 Hz independent of the molar mass. This correlation implies that finite size effects play a role in the β-relaxation. Figure 12 shows that the activation energy is not significantly modified by end-linking. Since for end-linked systems T_g increases weakly with the molar mass, one might expect, for a given temperature, a weak decrease of f_m. Instead, we observe a weak increase, showing that f_m is no longer correlated with T_g after end-linking.

Discussion

Like most polymers PPS does not have a dipole moment parallel to the chain backbone. This means that only the segmental relaxation is active in DS, while in

MS both the segmental and the conformational relaxation are observed. Figure 10 shows that for a given distance from the glass transition temperature ($T - T_{gv}$) the α-relaxation peak is systematically situated at a frequency 9 times larger in MS than in DS. The same difference was reported earlier for the precursors. The difference is at least partially due to fact that DS measures the response to a strain while MS measures the response to a deformation. MS therefore emphasizes faster modes, which leads to a larger value of f_m than in DS at the same temperature. The α-relaxation peaks in DS are much closer to those in MS in the different representation shown in Figure 8b, which also emphasizes the faster modes.

The amplitude of a relaxation mode in DS depends on the strength of the dipole moment that relaxes with this mode. It is therefore possible that the relaxation of the carbamothioate links is important in DS even if their volume fraction is small. A very large dipole moment of the carbamothioate links would lead to a strong signal in DS, but the effect on the mechanical relaxation could still be insignificant. This would explain why the additional α′-relaxation is observed in DS and not in MS. However, if this were the case the low-frequency dielectric permittivity (ϵ_0) should increase strongly with increasing volume fraction of carbamothioate links, i.e., with decreasing molar mass of the precursors. The end-linked samples are very viscous, and it is experimentally difficult to obtain precise reproducible values of ϵ_0. Nevertheless, within the rather large experimental error we do not observe an increase of ϵ_0 after end-linking ($\epsilon_0 = 8-9$ for all precursors and $\epsilon_0 \approx 5$, 12, 11, 9, and 9 for S1 to S5, respectively, after end-linking). There is certainly no sign of a very strong increase of ϵ with at low molar mass, which could explain the dominance of the α′-relaxation in terms of additional dipoles. We must therefore suppose that the α′-relaxation is due to a modified relaxation of chain backbone dipoles.

A coherent interpretation of the DS results is obtained by assuming that the mobility of a certain number of segments (n_m) near the carbamothioate links is reduced. It is reasonable to assume that n_m is the same for all samples, which implies that the fraction of the modified segments is inversely proportional to the molar mass of the precursors. n_m can be estimated from the relative strength of the two modes at different molar masses which gives $n_m \approx 15$. However, this interpretation does not explain why two distinct modes are observed and not a simple broadening of the peak together with a shift toward lower frequencies.

In ref 9 we reported a similar effect of end-linking in DS for PPO. For that system we could not tell whether the additional mode was due to modification of the perpendicular or the parallel component of dipole moment. PPS does not have a significant parallel component so that we can now conclude that the additional mode is not due to a modification of chain backbone conformational relaxation. A systematic study of the dielectric relaxation of end-linked PPO with range of precursors will be reported elsewhere.

If the α′-relaxation is due to the dipole relaxation PPS segments modified by carbamothioate links, one may wonder why do we not observe this relaxation in MS. Part of the answer is that in MS faster modes emphasizes the faster modes. But this cannot be the complete answer because transformation of the shear modulus data into the corresponding compliance data ($J''(\omega)$) which emphasizes slower modes does not reveal a distinct additional mode. In addition, even the different representation of the DS results reveals the α′-relaxation for the smaller samples. A better explanation is the limited frequency range in MS ($f < 20$ Hz). Figure 7 shows that for $f < 20$ Hz the two modes have merged into a single peak.

The β-relaxation is a common phenomenon in polymers, and in many cases one can identify a local motion of a particular molecular group, but in PPS and PPO there is no obvious candidate for such a localized mode. We observed a correlation between T_g and the β-relaxation for the precursors over a range of molar masses,[10] which suggests that the β- and α-relaxation are related. This conclusion was reinforced by a recent experiment in which we modified a small PPS by exchanging the SH terminal groups for OH groups.[15] The chemical modification leads to a strong increase of T_g due to the formation of hydrogen bonds. The activation energy of the β-relaxation is the same after modification, but the prefactor decreases in such a way that the correlation with T_g is preserved, which shows again that the β- and α-relaxation are related. Such a relation is not expected if the β-relaxation is caused by the localized motion of a specific molecular group. However, after end-linking the correlation of the β-relaxation with T_g is lost while, nevertheless, the shape and temperature dependence of β-relaxation are the same before and after end-linking. We are not aware of a model for the β-relaxation that is consistent with the experimental results presented here.

References and Notes

(1) Prochazka, F.; Nicolai, T.; Durand, D. *Macromolecules* **1996**, *29*, 2260.
(2) Tabellout, M.; Baillif, P. Y.; Randrianantoandro, H.; Litzinger, F.; Emery, J. R.; Nicolai, T.; Durand, D. *Phys. Rev. B* **1995**, *51*, 12295.
(3) Nicolai, T.; Randrianantoandro, H.; Prochazka, F.; Durand, D. *Macromolecules* **1997**, *30*, 5893.
(4) Randrianantoandro, H.; Nicolai, T.; Prochazka, F.; Durand, D. *Macromolecules* **1997**, *30*, 5897.
(5) Nicolai, T.; Prochazka, F.; Durand, D. *J. Rheol.* **1999**, *43*, 1511.
(6) Nicolai, T.; Floudas, G. *Macromolecules* **1998**, *31*, 2578.
(7) Randrianantoandro, H.; Nicolai, T. *Macromolecules* **1997**, *30*, 2460.
(8) Bauer, M. E.; Stockmayer, W. H. *J. Chem. Phys.* **1965**, *43*, 4319.
(9) Nicolai, T.; Prochazka, F.; Durand, D. *Phys. Rev. Lett.* **1999**, *82*, 863.
(10) Nicol, E.; Nicolai, T.; Durand, D. *Macromolecules* **1999**, *32*, 5893.
(11) Plazek, D. J.; Schlosser, E.; Schönhals, A.; Ngai, K. L. *J. Chem. Phys.* **1993**, *98*, 6488.
(12) Nicol, E.; Bonnans-Plaisance, C.; Levesque, G. *Macromolecules* **1999**, *32*, 4485.
(13) Britain, J. W.; Gemeinhardt, P. G. *J. Appl. Polym. Sci.* **1960**, IV, *11*, 207.
(14) Zuika, I. V.; Bankovskii, Yu. A. *Russ. Chem. Rev.* **1973**, *42*, 22.
(15) Nicol, E.; Durand, D.; Nicolai, T., unpublished results.

MA992063B